Title
Near-infrared catecholamine nanosensors for high spatiotemporal dopamine imaging.

Journal
Nature Protocols, 16(6)

Authors
Yang, Sarah
Del Bonis-ODonnell, Jackson
Beyene, Abraham
et al.

Publication Date
2021-06-01

DOI
10.1038/s41596-021-00530-4

Peer reviewed

HHS Public Access

Author manuscript

Nat Protoc. Author manuscript; available in PMC 2023 September 17.

Published in final edited form as:

Nat Protoc. 2021 June ; 16(6): 3026–3048. doi:10.1038/s41596-021-00530-4.

Near-infrared catecholamine nanosensors for high spatiotemporal dopamine imaging

Sarah J. Yang[1,6], **Jackson Travis Del Bonis-O'Donnell**[1,6], **Abraham G. Beyene**[2], **Markita P. Landry**[1,3,4,5,✉]

[1]Department of Chemical and Biomolecular Engineering, University of California, Berkeley, Berkeley, CA, USA.

[2]Janelia Research Campus, Howard Hughes Medical Institute, Ashburn, VA, USA.

[3]Innovative Genomics Institute (IGI), Berkeley, CA, USA.

[4]California Institute for Quantitative Biosciences, QB3, University of California, Berkeley, Berkeley, CA, USA.

[5]Chan-Zuckerberg Biohub, San Francisco, CA, USA.

[6]These authors contributed equally to this work: Sarah J. Yang, Jackson Travis Del Bonis-O'Donnell.

Abstract

Dopamine neuromodulation of neural synapses is a process implicated in a number of critical brain functions and diseases. Development of protocols to visualize this dynamic neurochemical process is essential to understanding how dopamine modulates brain function. We have developed a non-genetically encoded, near-IR (nIR) catecholamine nanosensor (nIRCat) capable of identifying ~2-μm dopamine release hotspots in dorsal striatal brain slices. nIRCat is readily synthesized through sonication of single walled carbon nanotubes with DNA oligos, can be readily introduced into both genetically tractable and intractable organisms and is compatible with a number of dopamine receptor agonists and antagonists. Here we describe the synthesis,

✉**Correspondence and requests for materials** should be addressed to M.P.L. landry@berkeley.edu.

Author contributions

A.G.B. and M.P.L. designed the experiments. J.T.D.B.-O. designed and built the microscope system and wrote the analysis software package. A.G.B., S.J.Y. and J.T.D.B.-O. performed the experiments. A.G.B., S.J.Y. and J.T.D.B.-O. analyzed the data and created the figures. S.J.Y. and J.T.D.B.-O. wrote the manuscript. All authors approved the manuscript.

Reporting Summary

Further information on research design is available in the Nature Research Reporting Summary linked to this article.

Code availability

Code for analyzing and processing nIR images is freely available online at https://github.com/jtdbod/Nanosensor-Imaging-App and released under an MIT license.

Competing interests

The authors declare no competing interests.

Additional information

Supplementary information The online version contains supplementary material available at https://doi.org/10.1038/s41596-021-00530-4.

Peer review information *Nature Protocols* thanks the anonymous reviewers for their contribution to the peer review of this work.

characterization and implementation of nIRCat in acute mouse brain slices. We demonstrate how nIRCat can be used to image electrically or optogenetically stimulated dopamine release, and how these procedures can be leveraged to study the effects of dopamine receptor pharmacology. In addition, we provide suggestions for building or adapting wide-field microscopy to be compatible with nIRCat nIR fluorescence imaging. We discuss strategies for analyzing nIR video data to identify dopamine release hotspots and quantify their kinetics. This protocol can be adapted and implemented for imaging other neuromodulators by using probes of this class and can be used in a broad range of species without genetic manipulation. The synthesis and characterization protocols for nIRCat take ~5 h, and the preparation and fluorescence imaging of live brain slices by using nIRCats require ~6 h.

Introduction

Dopamine plays a critical role in healthy brain function by orchestrating complex signaling processes ranging from learning to motor control[1–4]. Perturbations in dopamine signaling have been implicated in a number of neurodegenerative and psychiatric disorders, including Parkisons's disease, Huntington's disease and schizophrenia[5–7]. However, despite the central role of dopamine in brain health and disease, the mechanisms by which dopamine and other neuromodulators affect neurochemical brain function and malfunction are not well understood. Dopamine transmission is distinct from classical neurotransmission in its ability to shape the excitability of multiple neighboring neurons by diffusing beyond the synaptic cleft through a process known as volume transmission[8–10]. Understanding how this spread occurs spatially and temporally requires optical sensors capable of imaging dopamine at spatiotemporal scales (micrometers and milliseconds) commensurate with dopaminergic modulation[11].

Present methods of measuring dopamine dynamics are often limited in their temporal resolution or spatial resolution. Methods such as electrophysiology or genetically encoded voltage indicators can provide information on the electrical activity of dopaminergic neurons but cannot directly sense dopamine release from axonal boutons[12]. In contrast, methods taken from analytical chemistry, such as microdialysis and fast-scan cyclic voltammetry are able to directly quantify dopamine in the extracellular space[13]. Nevertheless, neither microdialysis nor fast-scan cyclic voltammetry can visualize dopamine in the extracellular space at the spatial and temporal resolution of single dopamine release sites (micrometers and milliseconds)[14–16]. Recently developed methods using genetically encoded dopamine receptor–based sensors (dLight and GPCR-activation-based dopamine sensors (GRABDA)) have begun to overcome existing challenges to measuring dopamine dynamics by introducing fast, optical sensors that directly sense dopamine[17,18]. These developments have underscored the immense value of imaging dopamine dynamics at fine spatiotemporal resolutions. However, the application of these sensors is limited to model organisms that are genetically tractable; furthermore, the structural similarities between genetically encoded dopamine sensors and endogenous dopamine receptors introduces cross-reactivity challenges when studying the effects of dopamine receptor agonists and antagonists commonly used as pharmacological agents.

Our development of a synthetic near-IR (nIR) catecholamine nanosensor (nIRCat) has provided a parallel, non-genetically encoded method for imaging dopamine modulation at the requisite spatiotemporal resolution of neurobiological relevance[19]. We show that nIRCat, synthesized from nIR fluorescent semiconducting single-walled carbon nanotubes, is a powerful catecholamine nanosensor that produces a 14-fold change in fluorescence at nIR wavelengths ideal for imaging in optically scattering brain tissues[20]. Via a rapid, simple and broadly applicable incubation procedure, nIRCat nanosensors readily image electrically or optogenetically stimulated dopamine release in living brain slices from standard mouse models (Charles River and Jackson Laboratories' C57BL/6 mice), disease-model mice and non-model organisms such as wild mice. Furthermore, nIRCat nanosensors work robustly in mice as young as 32 d and as old as 92 d and have been used successfully in both male and female mice. In contrast to genetically encoded dopamine sensors, nIRCat is compatible with dopamine pharmacology, enabling the study of how therapeutically relevant dopamine receptor agonists and antagonists shape dopamine modulation across the basal ganglia[19]. This protocol is useful for neuroscientists studying dopamine release in the basal ganglia, particularly those who seek to understand dopamine modulation in genetically intractable organisms or the impacts of dopamine receptor agonists and antagonists on neuromodulatory kinetics.

Overview of the procedure

In this protocol, we detail the use of nIRCat to image dopamine release in the dorsal striatum of ex vivo mouse brain slices (see Fig. 1 for a schematic overview). Synthesis of nIRCat is facile, entailing sonication of single-walled carbon nanotubes (SWNTs) with with ssDNA oligonucleotides composed of six guanine and thymine repeats (GT_6) followed by purification of nIRCat via centrifugation (Steps 1–5). After synthesis and purification, nIRCat can be characterized in in vitro solution-phase experiments to confirm and quantify its fluorescent response to dopamine (Steps 6–10) and reversibility to the binding and unbinding of dopamine (Steps 11–19). After characterizing nIRCat, the nanosensor is introduced ex vivo to live mouse brain acute slices. We provide a standard protocol for generating acute brain slices and a method for labeling the brain tissue with nIRCat through passive incubation (Steps 37–54). Labeled brain slices can be used to capture dopamine release evoked by both electrical and optogenetic stimulation. To image electrically evoked dopamine release, labeled brain slices are placed in an imaging chamber, continuously perfused with artificial cerebrospinal fluid (ACSF) and stimulated with an electrode (Steps 55–63). Conversely, for optogenetic stimulation, mice must be stereotaxically injected with adeno-associated virus (AAV) (Steps 20–36) and allowed 3 weeks to selectively express channelrhodopsin 2 (ChR2) in dopaminergic neurons before undergoing slice preparation and labeling (Steps 37–54). These channelrhodopsin-expressing axons then drive dopamine release into the striatum when stimulated by blue light (Step 60). Regardless of the stimulation mechanism, nIRCat-labeled slices can undergo drug washes to monitor changes in dopamine release and reuptake activity in response to therapeutically relevant dopamine receptor agonists and antagonists (Box 1). We also describe relevant video and data processing approaches for analyzing time series nIRCat image data with MATLAB code we uploaded to a public repository (Steps 64–74). Throughout this protocol, we identify parameters that can be modified for different experimental goals, and opportunities for

optimization. We also discuss how to troubleshoot common issues encountered during these procedures.

Applications and impact of the method

Among tools currently available for directly imaging dopamine modulation, nIRCat is unique in its high spatiotemporal resolution, compatibility with pharmacology and ability to be deployed in non-model organisms. The rapid fluorescence response of nIRCat nanosensors combined with their nanoscale size permits dopamine imaging in the brain extracellular space at spatiotemporal resolutions finer than microdialysis and at higher spatial resolution than fast-scan cyclic voltammetry[15,16]. In contrast to fluorescent protein-based dopamine sensors, the synthetic nature of nIRCat dramatically improves the dopamine probe's photostability because it is inherently non-photobleaching and thus indefinitely photostable[21]. nIRCat's nIR fluorescence can be readily multiplexed with other optical tools such as calcium or voltage indicators whose fluorescence resides in the non-overlapping visible wavelength spectrum. Furthermore, labeling living brain tissue with nIRCat is rapid and straightforward, requiring only passive incubation followed by washing and thus circumventing genetic manipulation. This passive labeling approach (i) avoids the necessity of working with genetically tractable organisms, (ii) avoids the use of AAV vectors to deliver the probe and (iii) bypasses the expression time required between probe administration and dopamine imaging. These features may be uniquely advantageous for researchers studying the role of dopamine in disease progression, allowing early-age and multiple time points to be sampled without the need to introduce additional genetic manipulation to a disease model. Finally, because the binding paradigm of dopamine to nIRCat is distinct from that of the native dopamine receptor, nIRCat does not optically respond to numerous dopamine receptor agonists and antagonists[22]. This pharmacological compatibility of nIRCat enables direct visual investigation of therapeutically relevant agents and their effects on dopamine modulation in the vicinity of its release sites.

This protocol describes the preparation and use of nIRCat to image dopamine release and reuptake in the dorsal striatum of acute mouse brain slices. We provide methods for probe preparation, in vitro solution-phase characterization, introduction into live brain slices and imaging in live brain slices. In addition, we discuss how the dynamics of dopamine release can be extracted from videos of nIRCat response. Notably, the methods described herein for probe synthesis and implementation are fundamentally generic for other carbon nanotube-based neuromodulator nanosensors, such as a recently developed probe for serotonin[23]. Therefore, our protocol will be of broad-scale utility to researchers wishing to image other neurochemicals as this toolkit expands. Lastly, the synthetic nature of nIRCat and other nanosensors of its class can be applied to any prepared live tissue without genetic manipulation, including brain tissue from different mouse lines or non-model organisms[19]. These adaptations of nIRCat for use in other organisms could enable neuromodulation research in organisms previously unexplored by the neurobiology research community.

Limitations

The three main limitations of nIRCat are the unique microscopy tools required for its implementation, its present verification only in acute brain slice preparations and its inability

to distinguish between the catecholamines dopamine and norepinephrine. Specifically, although nIRCat nanosensors possess a unique nIR spectral range within the tissue-transparency window, which does not overlap with optical neurobiological tools, imaging in the nIR requires specialized short-wavelength IR detectors that are less commonly available to neurobiology laboratories than visible microscopy[24]. Second, to date, SWNT-based nIR nanosensors have been used only to image dopamine, or other monoamines, in in vitro cell cultures, primary neurons and ex vivo brain slices[25,26]. There is presently no established method for in vivo imaging of dopamine with nIRCat, and more work must be done to use nIRCat within live animals[19]. Lastly, the molecular recognition site of nIRCat does not distinguish between dopamine and norepinephrine; therefore, nIRCat can be used as a dopamine probe in the context of brain regions or organisms absent of norepinephrinergic innervation, or alongside pharmacological agents for suppressing norepinephrine release[14,19]. As such, this protocol focuses on using nIRCat as a dopamine probe in the dorsal striatum, a brain region where dopamine is a key neuromodulator with minimal competing catecholamine release. Alternatively, nIRCat may be an attractive tool to use in organisms lacking norepinephrine signaling. One example is imaging dopamine modulation in *Drosophila melanogaster*, in which octopamine—known not to interfere with nIRCat fluorescence—replaces norepinephrine[19]. However, care must be taken in implementing nIRCat for imaging mouse brain regions such as the cortex where multiple catecholamine signals may be present.

Experimental design

nIRCat synthesis and characterization (Steps 1–19)—Synthesis of nIRCats occurs through dispersal of SWNTs with ssDNA oligonucleotides composed of six guanine and thymine repeats (GT_6) (Fig. 2a). This dispersal process is achieved through bath and probe tip sonication, which allows the GT_6 polymers to non-covalently adhere to the surface of the SWNT via π-π stacking interactions to form the nIRCat nanosensor[22]. The resulting individually dispersed semiconducting SWNTs exhibit intrinsic nIR fluorescence emission with peak wavelengths ranging from 900 to 1,500 nm depending on the chirality of the carbon lattice, a phenomenon absent from metallic nanotubes, nanotube bundles and multi-walled carbon nanotubes[21]. As such, effective sonication of the initial GT_6 and SWNT mixture is integral to successful synthesis of the nIRCat nanosensor (Fig. 2b). Similarly, centrifugation and recovery of the supernatant is also a key step that allows the successfully synthesized nIRCat nanosensor to be separated from the remaining, non-suspended SWNT (Fig. 2c). Some individual optimization around sonication time and starting SWNT to GT_6 ratio may be required to achieve efficient nIRCat nanosensor synthesis in individual laboratory conditions.

The adsorption of GT_6 to the SWNT surface not only aids the dispersal of the SWNT in aqueous solution, but also confers a catecholamine-selective increase in fluorescence to the nIRCat nanosensor. Robust performance of a nIRCat nanosensor in acute brain slices requires thorough in vitro solution-phase characterization to confirm a strong, catecholamine-specific fluorescence response and a fast, reversible fluorescence that changes with dopamine release and reuptake. Therefore, it is vital to test that the newly synthesized nanosensor shows a large increase in fluorescence when dopamine is added

exogenously to a wellplate containing the nanosensor (Fig. 3a). Nanosensor response should be tested for multiple dopamine concentrations ranging from 1 nM to 1 mM to ensure that the nanosensor shows a dynamic response to biologically relevant dopamine concentrations. Similarly, nanosensor reversibility should be tested by immobilizing the nanosensor in a microchannel and ensuring that the nanosensor increases and decreases in fluorescence as dopamine is washed into and out of the channel (Fig. 3d). It should be noted that before introducing a new drug wash experiment, all drugs should be tested alongside the nIRCat nanosensor in in vitro solution-phase experiments to ensure that the drug does affect the nanosensor fluorescence response or reversibility. For additional information on the preparation of DNA-SWNT dispersions and spectroscopic characterization for sensing, we refer the readers to previously published material from our group[22,27,28].

Imaging dopamine release in acute brain slices (Steps 20–54)—Introducing a nIRCat nanosensor into acute brain slices is a straightforward procedure that requires the acute brain slice to be passively incubated in ACSF containing 2 mg/l nIRCat nanosensor for 15 min (Fig. 4a,b). These incubation parameters have been determined experientially to produce well-labeled acute brain slices for imaging but may be adjusted to better serve individual experimental setups.

To specifically image dopamine dynamics without additional signal from other catecholamines, users should aim to image in the dorsal striatum, which is densely innervated by dopaminergic neurons from the substantia nigra pars compacta and lacks innervation from norepinephrine-releasing neurons. Dopamine release can be triggered by either electrical stimulation of brain tissue or by shining blue light on acute brain slices expressing channelrhodopsin (Fig. 4c)[29]. The most appropriate dopamine release method will vary on the basis of the desired experimental design. Although optogenetic release of dopamine allows for controlled, dopamine-specific release from specific cell types, it also requires that mice are injected with channelrhodopsin AAV roughly 3–4 weeks before imaging takes place. Conversely, electrical stimulation elicits general neuromodulator and neurotransmitter release but can be mobilized in both unmanipulated and genetically manipulated brain tissue. While in the dorsal striatum, dopamine release can be successfully driven by a single 1-ms pulse or a train of pulses. Users should note that electrical stimulation often results in the formation of bubbles at the electrode surface. At high stimulation strengths, these bubbles may deform the tissue, resulting in movement artifacts during data acquisition. To reduce these disturbances, it is suggested that users consider using lower-impedance electrodes (e.g., platinum over tungsten), perform experiments with shorter stimulation pulses or position the stimulator carefully into the tissue to prevent motion. Some motion artifacts can also be corrected through data processing procedures.

This protocol contains detailed procedures for the stereotaxic injection of AAV and preparation of live brain slices. Researchers seeking additional resources on how to conduct these procedures or adapt them to individualized experimental setups may reference similar protocols available through the *Journal of Visualized Experiments* with video walk-throughs[30,31]. Researchers are advised to note steps and reagents marked in this protocol as critical while comparing protocols.

Designing nIR-compatible microscopes—The characteristic nIR fluorescence of nIRCat precludes the use of typical silicon-based electron-multiplying charged-coupled devices (EMCCDs) or scientific complementary metal oxide semiconductor (sCMOS) cameras, which will not have a sufficient quantum efficiency in this wavelength range (900–1,450nm) to convert photons into electrons and generate a signal. In addition, commercial microscopy systems are not optimized to work in this wavelength range. As a result, attenuation of the nIRCat excitation source (typically, laser sources with peak emission of ~600–800 nm) as it traverses the illumination path and attenuation of the nIRCat nIR fluorescence as it traverses the imaging path toward the camera dramatically reduce signal and image quality. Constructing a home-built, wide-field, upright microscope with readily available optomechanics and lenses optimized for nIR imaging is a relatively affordable option that allows for full customization, optimization and control of the system (Fig. 5a,b). Moreover, integration of nIR imaging capabilities into an existing upright electrophysiology microscope through some modification is also possible[19]. Excitation light from a continuous-wave laser can be delivered via fiber optic coupling to the illumination port of an existing microscope and can illuminate the sample either through the objective lens from above (epi-illumination) or from below by using a condenser (trans-illumination). Ensure that anti-reflection coatings for lenses in either illumination path are optimized for nIR wavelength transmission and that any incompatible filters (e.g., heat filters) are removed where possible, although some attenuation and autofluorescence may be unavoidable. In addition, one must be aware of any clipping of the light source within the light path of the microscope that could attenuate the beam before it can be focused to the back focal plane of the objective. If attenuation of the excitation source cannot be avoided, then a higher-power laser should be used to offset the losses, provided it is still below the damage threshold of the other optical components. A sufficiently high-power light-emitting diode (LED) can be used as an alternative light source. We find that coupling the laser into a long (>5 m), large-bore (400 um), multimode fiber and projecting a magnified image of the fiber tip onto the back focal plane of the objective provides convenient and uniform illumination. Vibrating the fiber by attaching it to the perfusion vacuum pump is effective for reducing laser speckle.

Cameras fitted with indium gallium arsenide (InGaAs)-based detectors (commonly referred to as short-wavelength IR detectors by manufacturers) allow for the capture of the nIR photons emitted by nIRCats. Although few nIR detection options existed 10 years ago, there are now an assortment of companies designing and producing InGaAs cameras with specifications and features amenable to scientific and microscopic imaging. Relevant features include c-mount compatibility, large pixel area, hardware triggering, software development kit and application programming interface availability, thermoelectric cooling, low dark current and low read noise. In addition, some hybrid InGaAs sensors can detect visible photons as well as nIR photons, eliminating the need to manually switch between cameras for imaging in the traditional visible fluorescence range. We recommend testing nIR cameras from manufacturers to evaluate which is best suited for your laboratory’s particular system.

Choosing an appropriate objective is also critical for obtaining quality nIRCat images for quantitative analysis. The ideal objective should be a water-dipping physiology objective with a long working distance, high nIR transmission and aberration correction in the nIR range if possible. Contacting multiple manufacturers for specifications and testing demos is critical for choosing a suitable objective for your system. In addition, these objectives are compatible with other imaging techniques, such as laser scanning confocal, two-photon and super-resolution microscopy, reducing the up-front cost of modifying a microscopy system, although specific thread adapters and parfocal spacers may be required.

The main up-front cost for dopamine imaging with nIRCats is the high-sensitivity InGaAs camera, which can cost ~$30,000, although prices have continued to drop over the last several years. With this camera, modification of an existing electrophysiology rig can generate a system shared between multiple laboratories that is compatible for performing standard electrophysiology experiments alongside nIRCat imaging, potentially enabling new multimodal experiments. Alternatively, numerous manufacturers have released photomultiplier tubes and avalanche photodiodes with wavelength sensitivities compatible with nIRCat nanosensors with form factors that can be easily retrofitted into home-built laser scanning imaging systems for a substantially lower cost than a dedicated InGaAs camera.

Analyzing collected nIRCat time-series data (Steps 64–74)—The acquired time-series image data typically take the form of .tif files consisting of a stack of images arranged in $h \times w \times t$ pixel arrays, where $h \times w$ correspond to the image height and width and t corresponds to the frame number in the time series. Metadata, such as time stamps, can be included in the .tif file as a header or in a separate .txt or .xml file depending on the software used for image acquisition. For this reason, we recommend customizing and adapting analysis code that is optimized for both individual experimental procedures and the hardware and software used in each laboratory. In addition, organizing and storing data and subsequent analysis data into open source formats, such as HDF5 (The HDF Group, http://www.hdfgroup.org/HDF5), dramatically improve the organization and sharing of data both between laboratories and within the broader scientific community.

Similar to images of calcium indicators, dopamine release measured with nIRCat is quantified by calculating a change in fluorescence intensity of the nIRCats' $\Delta F/F_0$. Unlike calcium imaging, however, nIRCats occupy the extracellular space and not the cytosol or membrane of neurons. For this reason, the fluorescence microscopy images produced appear as irregular patterns, owing to the combination of dense axonal innervation and cell bodies comprising the neuropil where dopamine is released in striatal tissue. Without a ground truth morphological structure, such as a neuronal soma, or time-domain variance of activity (simultaneous evoked release), an alternative approach to image processing is needed than is typically used to process imaging data from calcium dyes[32,33]. To minimize bias and to reduce processing time for first-pass analysis by downsampling, select ROIs by defining a uniform square grid across the field of view (Fig. 5c). The physical ROI size can be user defined, although prior work suggests putative dopamine release sites on the order of 2 μm[19]; therefore, choosing a square grid with ROI sizes above this threshold is suggested. For each square ROI, a fluorescence time trace is used to calculate $\Delta F/F_0$, where F_0 is an

estimate of the underlying signal baseline (Fig. 5d,e). ROIs are identified as ‘inactive’ if their baseline fluorescence falls below a background threshold value or they do not exhibit a statistically significant transient after stimulation. From the remaining ROIs, relevant parameters, such as evoked peak height and decay constant, can be calculated. Extracting absolute reuptake rates from $\Delta F/F_0$ traces requires further deconvolution of the nanosensor kinetics. However, relative changes to peak release and reuptake times can be compared between brain regions or disease models or in response to pharmacological agents.

In this protocol, we outline a typical workflow for analyzing nIRCat data. We highlight points where alternative methods can be applied to better optimize analysis to suit the needs of a particular experiment or dataset. These processes can easily be automated for processing large batches of organized files to minimize user input time. We encourage the user to quantitatively evaluate multiple methods and tune parameters when analyzing their data and to share methods and code with the community through resources such as GitHub. A version of our analysis code is available at https://github.com/jtdbod/Nanosensor-Imaging-App.

Materials

Biological materials

- C57BL/6 mice, 10–20 weeks of age (Jackson Laboratory, stock no. 000664), but mice of the age, sex and type relevant to the researcher’s experiments can be substituted here—mouse lines that have previously been used successfully with nIRCat include C57BL/6 mice from Charles River Laboratories and wild *Mus spicilegus* mice **! CAUTION** Experiments involving mouse tissue must conform to institutional and national regulations. The animals and experiments used in this protocol have been approved by the Institutional Animal Care and Use Committee of the University of California, Berkeley. We encourage researchers to adhere to ARRIVE (Animal Research: Reporting of In Vivo Experiments) guidelines while designing animal experiments.

Reagents

nIRCat nanosensor synthesis

- SWNTs (NanoIntegris, raw small-diameter high-pressure carbon monoxide–synthesized SWNTs (HiPco)) **! CAUTION** Dry nanomaterials pose a respiratory health hazard when dispersed in air. Handle all dry nanomaterials in a powder or fume hood and dispose of all waste that comes in contact with nanomaterial as chemically hazardous waste. We find that adding a measured amount of water and ethanol to the dry SWNT dramatically improves handling and measuring ease ▲ **CRITICAL** This procedure is specific to HiPco synthesized, unpurified SWNT preparations. Differences in nanotube synthesis, catalyst, purification and manufacturer can modify the resulting nIRCat construct. Additional optimization of the DNA-SWNT ratio and suspension protocol are required for using other sources or preparations of semiconducting SWNTs.

- GT_6 DNA oligos, 1–2 mM stock solution in distilled water, stored at −20 °C (custom DNA oligo, standard desalting, sequence: GTGTGTGTGTGT; Integrated DNA Technologies, Inc.)

Optical characterization of nIRCat

- Dopamine hydrochloride (Millipore Sigma, prod. no. H8502)
- NaCl (Sigma-Aldrich, cat. no. S7653)
- (3-Aminopropyl)triethoxysilane (APTES) in Sure/Seal bottle (99%, CAS 919–30-2; Sigma-Aldrich, cat. no. 440140)
- 10× PBS (Corning, cat. no. 46–013-CM)

Stereotaxic injection of AAV

- Packaged AAV virus to be injected: For this protocol, we use pAAV-EF1a-double floxed-hChR2 (H134R)-EYFP-WPRE-HGHpA packaged in AAV1 (Addgene, cat. no. 20298-AAV1). The virus is produced at a concentration of $\geq 7 \times 10^{12}$ vg/ml as described by Addgene and the University of Pennsylvania Vector Core.
- Super glue (Loctite Gel Control Super Glue; Henkel, item no. 30379)
- 70% (vol/vol) ethanol (Fisher Scientific, cat. no. 02–002-804)
- Glycerol (Fischer Scientific, cat. no. 50–751-7538)
- Betadine solution (10% (vol/vol) povidone-iodine) (Fisher Scientific, cat. no. NC0158124)
- Meloxicam (10 mg/kg of animal)
- Lidocaine (2–4 mg/kg of animal) or bupivicaine (1–2 mg/kg of animal)
- Isoflurane (Sigma-Aldrich, CAS no. 26675–46-7)

Cutting buffer for acute brain slice imaging

- NaCl (Sigma-Aldrich, cat. no. S7653)
- $NaHCO_3$ (Sigma-Aldrich, cat. no. S5761)
- KCl (Sigma-Aldrich, cat. no. P9333)
- NaH_2PO_4 (Sigma-Aldrich, cat. no. S8282)
- $MgCl_2$ (Sigma-Aldrich, cat. no. 63069)
- Glucose, $C_6H_{12}O_6$ (Sigma-Aldrich, cat. no. G7528)
- Oxygen/carbon dioxide (95% O_2, 5% CO_2; carbogen) (Praxair, cat. no. BIOXCD5C-K)

Ascorbic acid-free ACSF for acute brain slice imaging

- NaCl (Sigma-Aldrich, cat. no. S7653)

- $NaHCO_3$ (Sigma-Aldrich, cat. no. S5761)
- KCl (Sigma-Aldrich, cat. no. P9333)
- NaH_2PO_4 (Sigma-Aldrich, cat. no. S8282)
- $MgCl_2$ (Sigma-Aldrich, cat. no. 63069)
- $CaCl_2$ (Sigma-Aldrich, cat. no. 21115)
- Glucose, $C_6H_{12}O_6$ (Sigma-Aldrich, cat. no. G7528)
- Oxygen/carbon dioxide (95% O_2, 5% CO_2; carbogen) (Praxair, cat. no. BIOXCD5C-K)

Preparation of acute brain slices

- Super glue (Loctite Gel Control Super Glue; Henkel, item no. 30379)
- Ice
- Ketamine (120 mg/kg)
- Xylazine (24 mg/kg)
- Isoflurane (Sigma-Aldrich, CAS no. 26675–46-7)
- Oxygen/carbon dioxide (95% O_2, 5% CO_2; carbogen) (Praxair, cat. no. BIOXCD5C-K)

Equipment

nIRCat nanosensor synthesis

- Glass beaker (VWR, cat. no. 75870–432)
- Microcentrifuge tubes (1.5 ml; VWR, cat. no. 89000–028)
- Well plate (384 well, polypropylene, natural; Greiner Bio-One, item no. 781201)
- Pipette tips (low-retention 10-, 200- and 1,000-µl filter tips; USA Scientific, cat. nos. 1181–3710, 1180–8710 and 1182–1730)
- Analytical balance (Radwag, AS 60/220.R2)
- Ultrasonic bath (Branson, cat. no. 15–336-100)
- Ultrasonic homogenizer with 6-mm tip (Cole-Parmer, cat. nos. UX-04711–70 and UX-04712–14)
- Tabletop centrifuge (Eppendorf, cat. no. 5418000017)
- 96-well microplate, polypropylene (Greiner Bio-One, item no. 655261) ▲ **CRITICAL** Ensure that your choice of well plate has minimal autofluorescence and absorbance in the nIR.

Optical characterization of nIRCat

- Vacuum gas manifold or Schlenk line with nitrogen source

- Tubing and luer connectors (fitting and tubing kit; Warner Scientific, LLC, product no. 64–1565)
- No. 1 microscopy cover glass (Fisher Scientific, cat. no. 12–542B)
- Microscope slides (VWR, cat. no. 16004–422)
- Self-adhesive flow cell microscope slides (sticky-Slide VI 0.4; Ibidi, GmbH, cat. no. 80608)
- Inverted microscope (Zeiss Axiovert)
- 100× total internal reflection fluorescence (TIRF) objective (Zeiss, alpha-plan Apochromat, 100×/1.46 Oil TIRF)
- Motorized microscope stage (Zeiss; Märzhäuser Wetzlar)
- Visible and nIR InGaAs camera (Raptor Ninox 640)
- nIR laser source and table mount (721 nm, 500 mW, continuous wave diode–pumped solid-state (CW DPSS) laser; OptoEngine, LLC)
- Fiber launch/alignment system (e.g., Thorlabs, KT110); Ø400 μm, 0.39 numerical aperture (NA), low hydroxyl ion (OH), FC/PC-FC/PC fiber patch cable, 5 m (Thorlabs, M74L05); two protected silver mirrors (PF10–03-P01); two kinematic mounts, posts and post holders (Thorlabs, KM100, PH2E, TR2 and CF125C); and illumination port adapter and optical cage components (Thorlabs, SM1A23)
- Short-wavelength IR spectrometer (Princeton Instruments, IsoPLane & PyLon 1024)
- 4f optics for coupling scope to spectrometer (Thorlabs, Achromatic doublets)
- Syringe pump (Harvard Apparatus, PHD200)

Stereotaxic injection of virus

- Glass capillary tubes (3.5 inch; Drummond Scientific Company, item no. 3–000-203-G/X)
- Micropipette puller (Sutter Instruments, model P-97)
- Sterile cotton swabs (Fisher Scientific, cat. no. 23–400-115)
- Sterile insulin syringes (Fisher Scientific, cat. no. 14–841-31)
- Monofilament nylon sutures (Ethilon, cat. no. 662G)
- Sterile scalpels (Daigger, cat. no. EF7281A)
- Sterile gloves (Ansell; VWR, 75872–022 (CS))
- Oxygen tank with appropriate regulator (k-tank; Praxair, cat. no. PX1321)
- Puralube ophthalmic ointment (Puralube, NDC 17033–211-38)
- Tissue adhesive (3M Vetbond; Fisher Scientific, cat. no. NC9259532)

- Stereotaxic frame and head restraint (World Precision Instruments, cat. no. 504926)
- Micromanipulator (MPC 200; Sutter Instruments, cat. no. MPC-385)
- Micro or dental drill (World Precision Instruments, cat. no. 503598)
- NanoJect applicator (Drummond Scientific Company, item no. 3–000-204)
- Clamping tweezers, surgical scissors and sterile scalpel
- Bead sterilizer (Germinator 500; Braintree Scientific, cat. no. GER5287)
- Electric razor (Conairs, cat. no. GMT175RD)
- Isoflurane vaporizer (VetEquip, item no. 901806)
- Homeothermic blanket (Harvard Apparatus, item no. 50–7221F)

Preparation of acute brain slices

- Filter paper (Whatman, cat. no. 1004 110)
- 5-ml syringe (Air-Tite, cat. no. 14–817-174)
- 19-gauge needle (Fisher Scientific, cat. no. 14815527)
- Single-edged razor blade (Fastenal, part no. 0267287)
- Microtome razor blades (Personna, double edge super blades; VWR, cat. no. 100491–888)
- 5-ml syringe (Air-Tite, cat. no. 14–817-174)
- Vibrating blade microtome, vibratome (Leica VT1200)
- Slice incubation chamber (Scientific Systems Design, Inc., BSK4)
- Low-volume slice incubation chamber (Scientific Systems Design, Inc., BSK2)
- Water bath (VWR, cat. no. 76308–830)
- Delicate scissors (VWR, cat. no. 82027–582)
- Large surgical scissors
- Metal spatula
- Hemostat dissecting forceps (VWR, cat. no. 10806–120)

Microscopy for and electrical stimulation of acute brain slices—▲ CRITICAL

The components listed below are required for the physiology microscope setup (Sutter Instruments or custom with Thorlabs/Cerna components). For a detailed description of the microscope setup, see Designing nIR-compatible microscopes under Experimental design.

- Visible and nIR InGaAs camera (500–600 nm: 40% quantum efficiency (QE); 1,000–1,500 nm: >85% QE; Raptor Photonics, Ninox 640)

- 900-nm long-pass filter and 45 degree dichroic mirror (Thorlabs, FELH900 and DMLP900R)
- 785-nm CW diode laser (OptoEngine LLC, MDL-III-785R-300mW)
- 473-nm CW diode-pumped solid state laser (Optoengine LLC, MBL-III-473–100mW)
- Arduino Uno R3 (www.arduino.cc)
- Fiber launch/alignment system (e.g., Thorlabs, KT110); Ø400 μm, 0.39 NA, low OH, FC/PC-FC/PC fiber patch cable, 5 m (Thorlabs, M74L05); two protected silver mirrors (PF10–03-P01); two kinematic mounts, posts and post holders (Thorlabs, KM100, PH2E, TR2 and CF125C); and illumination port adapter and optical cage components (Thorlabs, SM1A23)
- Anti-reflective-coated plano convex lenses or achromatic doublets for beam expansion optics (Thorlabs)
- 4×, 10× and 60× objectives with >60% transmission from 1,000 to 1,400 nm (Nikon, Plan Fluor 4×/0.13, NikonPlan Fluor 10×/0.30W WD3.5, Nikon CFI series NIR Apo 40×/0.8W DIC N2 WD3.5 and 60×/1.0 W differential interference contrast (DIC) N2 WD2.8)
- Infinity-corrected tube lens for custom microscope builds (e.g., Thorlabs, TTL200-S8)
- Thread adapters for objectives and ports, SM1-Olympus (Thorlabs)
- Micromanipulator for electrode placement (Sutter Instruments, MPC200; Scientifica PatchStar)
- Stage (Sutter Instruments; Thorlabs PLS-XY, MP150-RCH2 modified with Thorlabs components)
- Perfusion pump (World Precision Instruments, Peri-Star Pro)
- Perfusion bath (Warner Instruments SA-OLY/2-AL, P1/PH1, RC-26GLP; Scientifica LLC, slice recording chamber kit)
- Aspirator pump (Warner Instruments, drain waste vent (DWV) vacuum kit; house vacuum with Büchner flask + hydrophobic filter)
- Tissue harp (Warner Instruments)
- Inline heater with feedback control (Warner Instruments, TV-324C)
- Electrical signal sequencer and/or pulse generator (Molecular Devices, Axon Digidata 1440A; A.M.P.I., Master-8)
- Electrical isolator and stimulator (A.M.P.I., Iso-Flex)
- Tungsten bipolar microelectrode (Microprobes, WE3ST30.1A5)
- BNC cables and BNC terminal connectors

- Wire, pin connectors and heat shrink

Software

- Micro-Manager (https://www.micro-manager.org)
- Clampex 10.7 (Molecular Devices, www.moleculardevices.com)
- Arduino IDE and Micro-Manager configuration (www.arduino.cc, https://micro-manager.org/wiki/Arduino)
- Nanosensor imaging app (https://github.com/jtdbod/Nanosensor-Imaging-App)
- ImageJ (https://imagej.net)
- FIJI (https://imagej.net/Fiji)
- MATLAB (https://www.mathworks.com/products/matlab.html)
- Python 3.8.5 (https://www.python.org)
- numpy (https://numpy.org), scipy (https://scipy.org), matplotlib (https://matplotlib.org), scikit-image (https://scikit-image.org) and Jupyter Notebook (https://www.jupyter.org)

Reagent setup

Ascorbic acid–free cutting buffer—Add reagents to 1 liter of deionized water to final concentrations of 119 mM NaCl, 26.2 mM $NaHCO_3$, 2.5 mM KCl, 1 mM NaH_2PO_4, 3.5 mM $MgCl_2$ and 10 mM glucose. $CaCl_2$ is omitted from the cutting buffer. Bubble solution with oxygen/carbon dioxide (95% O_2, 5% CO_2; carbogen) for 15 min. The solution should be stored at 4 °C overnight and used within 36 h. ▲ **CRITICAL** Standard cutting buffer often contains ascorbic acid. It is important to use ascorbic acid–free cutting buffer during preparation for nIRCat imaging because ascorbic acid can attenuate the nIRCat nanosensor optical response.

Ascorbic acid-free ACSF—Add the following reagents to 2 liters of deionized water to final concentrations of 119 mM NaCl, 26.2 mM $NaHCO_3$, 2.5 mM KCl, 1 mM NaH_2PO_4, 1.3 mM $MgCl_2$, 10 mM glucose and 2 mM $CaCl_2$. Bubble solution with oxygen/carbon dioxide (95% O_2, 5% CO_2; carbogen) for 15 min. The solution should be stored at 4 °C overnight and used within 36 h. ▲ **CRITICAL** Standard ACSF often contains ascorbic acid. It is important to use ascorbic acid–free ACSF during nIRCat imaging because ascorbic acid can attenuate the nIRCat nanosensor optical response.

Equipment setup

Micropipettes for stereotaxic injections—Insert and secure a glass capillary tube with inner and outer diameters compatible with the Nanoject. Enter the following settings: Temp: 510, Pull: 60, Velocity: 60 and Time: 250 and then press the <PULL> button. Carefully remove the two resulting micropipettes. Break the tip of each micropipette by gently piercing a taught Kimwipe.

Procedure

nIRCat nanosensor synthesis ● Timing 1–2 h

! CAUTION Dry SWNT powder is hazardous and should be used in a fume hood or, preferably, a high-efficiency particulate air (HEPA)-filtered powder hood. Handling dry SWNT powder can be challenging because of static electricity and convective airflow. An anti-static gun or bracelet, or adding a known mass of deionized water to the SWNT powder, can ease handling.

! CAUTION All waste containing SWNTs should be collected and disposed of as hazardous chemical waste following proper guidelines established by your institution.

1. Prepare an SWNT-DNA solution by combining 1 mg of GT_6 DNA, ~1 mg of SWNT and NaCl solution to a 2-ml microcentrifuge tube. Add deionized water to bring the total volume to 1 ml and the final concentration of NaCl to 0.1 M. The nanotubes should remain insoluble at this step.

   ▲ **CRITICAL STEP** SWNT powder can be handled more easily if it is first mixed with water to form a slurry or cake of a known mass ratio. Sonicate briefly with a bath sonicator to disperse any hard pellets of SWNT.

2. Probe tip sonicate the above SWNT-DNA solution while placing the microcentrifuge tube in an ice bath for 10 min. For a 3-mm probe tip, set the amplitude of the driver to achieve a power output of 2–5 W (e.g., 50% amplitude). The solution resulting from sonication should appear dark black.

   ▲ **CRITICAL STEP** Ensure that the probe tip does not touch the sides of the microcentrifuge tube by clamping the tube in place. The probe tip should sit roughly halfway between the surface of the solution and the bottom of the tube (Fig. 2b).

   ▲ **CRITICAL STEP** The degree of functionalization depends on the properties of the particular batch of SWNT, DNA/SWNT conjugation ratios and variations in sonication intensity between probe tip sonicators. Differences in functionalization can quantitatively alter the fluorescence response of nIRCats to dopamine. Therefore, we recommend that users optimize mass ratios of DNA and SWNT and the sonication protocols to maximize nIRCat dopamine response.

3. Remove the sample from the ice bath and allow it to rest for 30 min at room temperature (20–25 °C).

4. Centrifuge the nIRCat solution with a benchtop centrifuge for 90 min at ~16,000*g* at room temperature. Remove and retain the top 90% of the supernatant, being careful to avoid perturbing the black pellet of insoluble SWNT aggregates. Discard the pellet (Fig. 2c).

   ? TROUBLESHOOTING

5. Quantify the concentration of dispersed SWNT in the nIRCat sample by collecting the absorbance spectrum by using a spectrophotometer or Nanodrop.

Calculate the nIRCat concentration by measuring the absorbance of the sample at 632 nm and using Beer's Law with an extinction coefficient $\varepsilon = 0.036$ L/(mg × cm) for raw HiPCO SWNTs[34].

▲ **CRITICAL STEP** Use an appropriate dilution of the nIRCat solution to fall within the linear range needed to apply Beer's Law, as required by your particular instrument; the target optical density of a sample dilution should be <1 OD.

▲ **CRITICAL STEP** The extinction coefficient varies depending on the manufacturing process of SWNT (e.g., HiPCO versus cobalt–molybdenum catalyst (CoMoCat)), relative proportions of chirality populations and type of polymer or surfactant used in the suspension. Any adaptations of this protocol require empirically deriving an extinction coefficient or using a relative, rather than an absolute, absorbance measurement to keep concentrations consistent.

■ **PAUSE POINT** The GT_6-SWNT nIRCat suspension can be stored at 4 °C for ≤1 month. For samples older than 1 month, we recommend testing the nIRCat fluorescence response to dopamine in in vitro solution-phase experiments (as described in Steps 6–10) to ensure nanosensor viability and consistency. For larger experiments, we also recommend scaling up the synthesis as needed.

Validating and quantifying nIRCat dopamine response ● Timing 1–2 h

6. Prepare a 5-mg/l dilution of nIRCat in 0.1 mM NaCl and add ~100 μl of this nIRCat dilution to a 96-well plate (Fig. 3a).

7. Collect the fluorescence emission spectrum by using a plate reader outfitted with an InGaAs detector, nIR diffraction gratings and an nIR light excitation source (e.g., 721-nm CW laser). Confirm the presence of characteristic nIRCat fluorescence emission peaks at ~990, 1,040, 1,075, 1,130 and 1,200 nm (Fig. 3b). Note that different peak intensities may arise in the nIRCat fluorescence spectrum if using a different excitation source.

8. To validate and quantify nIRCat's dopamine response, add 10% (vol/vol) of freshly made 1 mM dopamine-HCl solution to the well containing nIRCat, mix thoroughly by pipetting up and down a few times and then record a new nIRCat fluorescence spectrum. Repeat in at least triplicate. Using MATLAB or Python as the tool of choice, calculate the fold-change in fluorescence, $\Delta F/F_0 = (F - F_0)/F_0$, by integrating the fluorescence emission spectrum before (F_0) and after (F) adding dopamine (Fig. 3b).

▲ **CRITICAL STEP** The dopamine solutions will oxidize over time and exposure to light. Prepare fresh batches of different dopamine concentrations and repeat the above process to test nIRCat's fluorescence response as a function of dopamine concentration.

▲ **CRITICAL STEP** Adding different long-pass filters on the imaging microscope can change the effective $\Delta F/F_0$ because different peak emissions

of nIRCat respond differently to dopamine. For example, using a 1,080-nm long-pass filter will produce higher $\Delta F/F_0$ than a 900-nm long-pass filter because nanotubes with shorter emission wavelengths exhibit a lower response to dopamine and contribute to a larger background fluorescence.

? TROUBLESHOOTING

9. To test the selectivity of nIRCat, repeat the above experiment for a panel of analytes or drugs of interest (e.g., catecholamines, dopamine agonists and antagonists and dopamine transporter blockers).

? TROUBLESHOOTING

10. Prepare aliquots of dopamine-HCl titrations in 0.1 M NaCl ranging from 1 nM to 1 mM. Repeat Step 8 in separate wells containing 2 mg/l nIRCat. Wait 30 min after the addition of dopamine before measuring the nIRCat fluorescence response spectra. Using MATLAB or Python as the tool of choice, fit an equilibrium binding and calibration curve $\frac{I-I_0}{I_0} = \alpha\frac{[\mathrm{A}\theta]}{[\theta_{\mathrm{tot}}]} + B = \alpha\frac{([\mathrm{A}]K_{\mathrm{A}})^n}{([\mathrm{A}]K_{\mathrm{A}})^n+1} + B$ and calculate the equilibrium binding constant.

Imaging individual nIRCats and confirming reversibility ● Timing 1–2 h

11. Clean a rectangular #1.5 glass coverslip (e.g., 50 × 22 mm) with alcohol or mild detergent, rinse with deionized water and then blow dry with nitrogen.

12. Prepare a positively charged surface on the glass coverslip by functionalizing the coverslip with APTES. To do so, incubate the coverslip in ethanol containing 10% (vol/vol) APTES for 5 min. Rinse the coverslip with deionized water and blow dry with nitrogen.

! CAUTION APTES is toxic, caustic and sensitive to moisture and oxygen. Use APTES only in a fume hood with appropriate personal protective equipment.

▲ **CRITICAL STEP** APTES stock solution degrades rapidly over time when used outside of a glove box. To reduce degradation, use a Shlenk line and appropriate techniques for handling air-sensitive materials. If a Shlenk line is not available, preparation of APTES solutions in ambient conditions can still enable proper functionalization of the class slide; however, the stock of APTES will need to be replaced more frequently.

13. Affix an Ibidi sticky-Slide VI 0.4 to the functionalized coverslip to produce a flow cell with six microchannels.

14. Flush a channel with 100 µl of PBS by pipetting PBS into a well on one side of the channel or by using a syringe pump and luer lock fittings.

15. Remove excess buffer from the well and immediately add 50 µl of a 5-mg/liter nIRCat solution. Remove any buffer accumulated in the downstream well to

ensure that the solution flows through the channel. Incubate for 5 min at room temperature.

16. Rinse the channel three times with 50 μl of PBS.

▲ **CRITICAL STEP** Ensure that the channel does not dry out.

17. Image the surface-immobilized nIRCats toward the center of the channel by using an inverted epifluorescence microscope outfitted with a 100× oil immersion objective, nIR excitation laser and high-sensitivity InGaAs camera (Fig. 3c).

18. Fill a reservoir of the flow channel with PBS and pump this buffer through the channel at a volumetric flow rate of 40 μl/min. When the liquid in the reservoir is nearly depleted, add 40 μl of 10 μM dopamine-HCl in PBS and then begin acquiring a time series image while driving the solution through the channel at a flow rate of 40 μl/min. As the dopamine solution is drawn into the channel, an increase in the fluorescence of surface-immobilized nIRCats should be observed. Repeat again by flowing PBS through the channel to observe a decrease in nIRCat fluorescence as dopamine is removed from the channel (Fig. 3d).

▲ **CRITICAL STEP** nIRCat can become dislodged from the surface if the flow rate is too high. Adjust as necessary.

19. Quantify the fluorescence change of individual nIRCats as a function of time by drawing a selection box around individually imaged nIRCats and using the *Image* → *Stacks* → *Plot Z-Axis Profile* feature of FIJI or ImageJ[35,36] or by using tools available in MATLAB or Python libraries, such as scikit-image[37]. A nIRCat fluorescence-versus-time trace that shows a repeatable step in fluorescence as dopamine is washed on and off should be observed.

Preparation of mice for optogenetic dopamine release ● Timing 2–3 h (3–4-week protein-expression period)

20. Sterilize all tools in the bead sterilizer and place tools in a designated sterile area. Put on sterile gloves.

! CAUTION Ensure that recently sterilized tools have had enough time to cool to room temperature after sterilization before use.

21. Anesthetize the mouse with 3–5% (wt/vol) isofluorane. (Mice were group-housed after weaning at postnatal day 21 and kept with nesting material on a 12:12 light cycle.)

! CAUTION Ensure that all experiments are in line with applicable institutional and national guidelines for animal housing and surgery. Experiments should be approved by the Institutional Animal Care and Use Committee.

22. Once the mouse is deeply anesthetized and no longer responds to the administration of a toe pinch, reduce the isoflurane to 1.5% (wt/vol). Throughout the surgery, regularly check the animal's depth of anesthesia via toe pinch and adjust the level of isoflurane appropriately.

23. Administer an analgesic cocktail of lidocaine (2–4 mg/kg) and meloxicam (10 mg/kg) subcutaneously for post-operative care. Shave off the fur in the triangular area between the animal's ears and eyes. Apply ophthalmic ointment to both eyes.

24. Position the animal in the stereotaxic frame, inserting ear pieces and aligning the animal's head to be level as necessary.

25. Using a sterile cotton tip applicator dipped in ethanol, clean the shaved area in a spiral motion. Follow this protocol with a cotton tip applicator dipped in betadine.

26. Repeat the ethanol and betadine cleaning two more times as described in Step 25.

27. Using a sterile scalpel, make an incision down the midline of the animal's head, starting from between the eyes and moving down toward the ears. Expose the skull.

28. Identify the bregma and lambda under a stereoscope.

29. Load 0.5 μl of the double floxed-ChR2-EYFP AAV virus into the autoinjector and align the injector by using the relevant coordinates (for substantia nigra pars compacta, −3.08 mm from bregma, 1.25 mm lateral from midline and 4.0 mm vertical from cortical surface).

30. Inject the virus slowly at a rate <100 nl/min.

31. Wait 1 min before slowly retracting the needle from the brain.

32. Repeat the injection (Steps 29–31) on the other hemisphere if injecting bilaterally.

33. Close the skin above the skull and suture the incision closed.

34. Place the animal back into the home cage that is positioned halfway onto a heating pad. Monitor the animal until normal breathing and alertness are restored.

35. Twelve hours after the original injection of meloxicam (Step 23), provide a secondary injection of meloxicam (10 mg/kg) subcutaneously.

    ▲ **CRITICAL STEP** Monitor the animal to ensure that there is no irritation or inflammation from the surgery.

36. Allow 2–3 weeks for the virus to express before imaging.

Preparation of acute brain slices and nIRCat brain tissue labeling ● Timing 2–3 h

37. Prepare ACSF and cutting buffer the night before or the morning of imaging and cool down to 4 °C (see Reagent setup). Bubble the cutting buffer with carbogen for 30 min before freezing the solution into a slush at −70 °C. Begin bubbling ACSF in the slice collection chamber with carbogen in a 37 °C water bath.

38. While the cutting buffer is freezing, gather ice, a syringe and a needle by the vibratome. Place a fresh blade into the vibratome and place ice around the vibratome cutting chamber.

39. When the cutting buffer is partially frozen (~20 min if previously stored at 4 °C), remove from −70 °C and use a large spatula to 'mash' any solid ice chunks into a fine, uniform slush. Pour half of the slush into an extraction chamber and begin bubbling the extraction chamber with carbogen. Keep the remainder of the cutting buffer bubbling with carbogen on ice. Immediately before Step 40, fill the 5-ml syringe with ice-cold cutting buffer and expel any bubbles within the syringe and needle by pushing out the plunger.

40. Deeply anesthetize the animal via intraperitoneal injection of ketamine (120 mg/kg) and xylazine (24 mg/kg). When the animal no longer responds to a hard toe pinch, open the animal's thoracic cavity with the dissection scissors and transcardially perfuse the animal by injecting ice-cold cutting buffer into the right ventricle of the heart and snipping the left atrium to allow blood to exit. The injection should be at a rate of ~5 ml over 2 min.

41. Following perfusion, decapitate the animal with scissors and peel back skin to expose the skull while submerging the skull in an ice-cold cutting buffer solution in the extraction chamber. Remove the cerebellum by using either scissors or a razor blade, taking care to create a flat surface at the caudal end of the brain for mounting (Fig. 4a).

42. Using dissection scissors, cut across the olfactory bulb and then cut carefully up the middle and around the sides of the skull to form two large skull pieces. Take care not to accidentally nick the brain while cutting through the skull. Using tweezers, carefully maneuver the tweezers between the skull and brain so that the tweezer tips lie approximately in the middle of the skull piece. Lift the skull piece upward off the brain (Fig. 4a).

    ▲ **CRITICAL STEP** Keep the skull and brain submerged in the cold cutting buffer during the extraction process. Rapid extraction (<1 min) minimizes deterioration of the tissue and increases slice viability.

43. Using a small spatula, carefully maneuver the brain out of the skull and into the extraction chamber.

44. Prepare the vibratome cutting chamber by filling it with cutting buffer liquid (not ice chunks) and surrounding the chamber with ice. Place a layer of super glue onto the mounting stage.

45. Carefully move the brain onto a flat spatula and quickly and gently dab the flat base with clean Whatman filter paper. Lower the flat caudal end of the brain onto the glue to mount the brain onto the mounting stage.

46. Quickly transfer the mounting stage into the vibratome cutting chamber and bubble the brain with carbogen.

47. Prepare 300-μm coronal sections until the corpus callosum visible in each hemisphere appears to fuse at the midline. Collect the next one to three acute slices of the anterior striatum containing the caudate, putamen and nucleus accumbens or until the anterior commissure appears to fuse at the midline.

? TROUBLESHOOTING

48. Use a wide-mouthed transfer pipette to collect coronal slices containing the dorsal striatum and transfer the slices into ACSF in the slice collection chamber at 37 °C. Keep slices at 37 °C for 30 min.

49. Remove the slice collection chamber from the water bath and let it sit at room temperature for 30 min.

50. To label the slice with nIRCat, begin by bubbling ACSF at room temperature in a separate incubation chamber with carbogen. Using a transfer pipette, move the slice to be labeled into the incubation chamber.

▲ **CRITICAL** If using a full brain slice instead of a hemisphere, it can be helpful to make a small nick outside of the striatum to remember which face of the slice is labeled.

51. Calculate the volume of nIRCat necessary to bring the incubation chamber to a concentration of 2 mg/liter nIRCat (dependent on the concentration of nanosensor stock and the size of the incubation chamber).

52. Load stock nIRCat into a pipette at a volume calculated in Step 51 and move the tip just into the ACSF solution. Without touching the tissue, discharge the concentrated nIRCat into the incubation chamber while moving the tip around above the brain tissue. Let the slice incubate in the bubbling ACSF-nIRCat solution for 15 min. The side of the slice facing upward will be most strongly labeled with nIRCat, and this side should be used during subsequent imaging (Fig. 4b).

53. Fill three wells in a 16-well plate with ACSF. After the slice has finished incubating, wash excess nanosensor off the slice by transferring it between the three wells by using a transfer pipette.

54. Move the slice onto a microscope or into carbogen-bubbled ACSF at room temperature and let rest for 15 min.

Imaging evoked dopamine release in acute brain slice ● Timing ~1 h per acute brain slice

55. Prepare the microscope for imaging by flowing ACSF bubbled with carbogen through the microscope perfusion chamber. Turn the imaging chamber's temperature control on and set the perfusion chamber temperature to 37 °C. Turn the microscope micromanipulator and sequence generator on. Attach a new bipolar stimulation electrode to the micromanipulator handle and connect the leads to the stimulation isolator unit (Fig. 4c).

56. Using a transfer pipette, move the nIRCat-labeled slice into the microscope perfusion chamber. Take care that the strongly labeled face of the slice is facing upward toward the microscope objective. Gently place a harp on top of the slice to prevent it from moving during imaging.

▲ **CRITICAL STEP** Take care to keep the nylon harp strings away from your targeted imaging area to avoid shearing tissue and nanosensor from the slice.

57. Using the 4× objective, position and focus the region of striatum to be imaged (dorsolateral, dorsomedial, etc.) so that it is visible on the microscope camera. If performing electrical simulation, use the micromanipulator to lower the bipolar stimulation electrode to just above the targeted field of view so that the electrode is above but not touching the brain slice. If desired, record the coordinates of the field of view on the slice or capture an image of the electrode position relative to the entire brain slice.

58. Switch to the 60 × water-dipping objective and zero the micromanipulator at the tip of the electrode to mark the field of view coordinates. For electrical stimulation, move the bipolar electrode 150–200 μm away from the field of view, ensuring not to make contact with the surface of the slice. Bring the bipolar electrode into contact with the slice by gently lowering it to the top surface of the brain slice and return to the original field of view.

59. Un-shutter the nIR laser and adjust the intensity to balance the grayscale pixel histogram by placing the histogram peak between 50% and 75% of the camera's true bit depth while avoiding saturating pixels.

▲ **CRITICAL STEP** Wait 1 min before beginning time series data acquisition and stimulation to ensure that the slice is stable in the bath and that the fluorescence signal has stabilized.

? TROUBLESHOOTING

60. For electrical stimulation, connect the stimulation isolator to the pulse generator by using a Bayonet Neill–Concelman (BNC) cable and appropriate adapter. For optogenetic stimulation, connect the transistor transistor logic (TTL) trigger of the 473-nm laser to the pulse generator.

? TROUBLESHOOTING

61. Using Micro-Manager or other software, begin image acquisition and timed stimulation. Images should be acquired at frame rates of 9 frames/s (nominal) for 600 frames, or however many frames the RAM configuration on the computer allows. Electrical or optical stimulation should be triggered by software after collecting enough frames of baseline activity to establish a baseline fluorescence signal (e.g., 200 frames).

62. After acquisition finishes, shutter the nIR laser. Wait 2–5 min before beginning the next acquisition. To adapt this protocol to include drug washes, see the suggested protocol in Box 1.

63. When the experiment concludes, rinse the perfusion system and water-dipping microscope objective with distilled water.

Processing time series nIRCat imaging data ● Timing 2–3 h

The steps below outline the typical data analysis pipeline for processing image stacks obtained by using the above methods. These steps are automated in a MATLAB app available at https://github.com/jtdbod/Nanosensor-Imaging-App or can be easily adapted into Python scripts by using matplotlib, numpy, scipy and scikit-image packages.

64. Load the .tif stack into memory by using analysis software (e.g., ImageJ/FIJI, MATLAB or Python).

65. (Optional) Perform motion correction on the time series image stack (e.g., the StackReg plugin in FIJI).

▲ **CRITICAL STEP** Even after correcting for motion, artifacts related to motion, such as from electrical stimulation, can still produce fluorescence intensity artifacts. Data should be periodically audited and hand-checked by a user. Time series traces with excessive motion artifacts should be discarded or cropped before processing.

66. Generate a median projection image by calculating the median intensity value across all frames for each pixel in the image stack. Alternatively, the average intensity value or 95th percentile can be used.

67. Define ROIs by dividing the image frame into equal-sized square ROIs of a size, in pixels, specified by the user. Number each ROI sequentially.

68. Eliminate ROIs within the time-projected image where minimal fluorescence is detected. The criteria for removal can be determined by estimating the background intensity level of the image with a threshold value calculated by using standard methods, such as Otsu's method[38].

69. Load the first frame of the time series and perform desired preprocessing. For example, median spatial filtering is commonly used to remove noise in images resulting from dead or gain-sensitive saturated pixels.

70. For each remaining ROI, calculate mean pixel intensity, coordinates, shape and any other metrics relevant to your experiment.

▲ **CRITICAL STEP** These calculations can be done by using a 'for loop'; however, there are many packages available that can implement this step by using lower-level implementations, such as C/C ++, to dramatically reduce computational time. Examples include regionprops() in MATLAB or skimage.measure.regionprops() in Python.

71. Calculate each ROI $\Delta F/F_0 = (F(t) - F_0(t))/F_0(t)$, where $F(t)$ is the mean fluorescence value of a given ROI at time t, and $F_0(t)$ is the drifting baseline of the signal calculated by using a median filter with a window 25 × greater than

the expected transient time and truncating the window size at the beginning and end of the trace.

▲ **CRITICAL STEP** The baseline fluorescence signal drift can be attributed to tissue drift, artifacts entering the field of view of the bath, motion and shadow artifacts caused by electrolysis at the electrode, tissue slice regions moving in and out of focus, desorption or degradation of the nIRCat nanosensor. Median filtering is chosen to estimate this baseline because it minimally affects the shape of the fluorescence trace, which is critical for fitting and extracting parameters such as the dopamine reuptake constant[39]. The window size may need to be adjusted depending on the type of experiment and quality of fluorescence signal. Alternative methods include spectral filtering and percentile filtering. The baseline signal can also be used to flag ROIs for removal if artifacts introduced obscure the true fluorescence transients.

72. Determine if a statistically significant fluorescence transient occurs for each ROI by estimating the baseline noise level and its standard deviation, σ, from the distribution of negative transients of the $\Delta F/F_0$ trace. If the signal, $\Delta F/F_0$, rises to $>3\sigma$ within 1 s of stimulation, designate the trace and ROI as significant[32].

73. For each ROI containing a significant transient, calculate parameters relevant to the performed experiment, including (i) time-to-peak after stimulation, (ii) peak amplitude, (iii) signal duration, (iv) total integrated signal and (v) decay constant. Estimate the decay constant, τ of the signal by fitting the equation $F(t) = \alpha[1 - \exp(-t/\beta)] \times \exp(-(t - \gamma)/\tau)$ by using a nonlinear solver package in MATLAB/Python (e.g., lsqcurvefit()).

74. Store measured parameters in an appropriate data structure to enable downstream processing for plotting ensemble or experimental averages. A sample video of nIRCat fluorescence upon electrical stimulation is provided in Supplementary Video 1, and a sample video of nIRCat $\Delta F/F$ upon electrical stimulation after image processing is provided in Supplementary Video 2.

Troubleshooting

Troubleshooting advice can be found in Table 1.

Timing

Steps 1–5, nIRCat nanosensor synthesis: 1–2 h

Steps 6–10, validating and quantifying dopamine response: 1–2 h

Steps 11–19, imaging individual nIRCats and confirming reversibility: 1–2 h

Steps 20–36, preparation of mice for optogenetic dopamine release: 2–3 h plus 3–4-week protein-expression period

Steps 37–54, preparation of acute brain slices and nIRCat brain tissue labeling: 2–3 h

Steps 55–63, imaging evoked dopamine release in acute brain slices: ~1 h per acute brain slice Steps 64–74: processing time series nIRCat imaging data: 2–3 h

Box 1, imaging in brain slice by using drug washes: ~1 h per acute brain slice

Anticipated results

We expect that this protocol will enable researchers to synthesize and characterize nIRCat nanosensors and subsequently use nanosensors to label the extracellular acute brain slice for quantifying dopamine release. This protocol outlines the techniques necessary to synthesize nIRCat nanosensors for optical dopamine sensing, quantify their fluorescence emission and absorbance spectra and confirm the magnitude and reversibility of dopamine response of individual nanosensors (Fig. 3). In addition, these details provide the reader with the necessary tools to explore synthesis space by using different polymer wrappings to refine properties such as binding kinetics and optical response as well as develop SWNT-based nanosensors for different targets.

NIR imaging of labeled slices can be electrically or optically (with genetically expressed opsins, e.g., ChR2) stimulated to evoke dopamine release that is monitored via local changes in fluorescence intensity. These image time series can be analyzed to identify regions where dopamine release occurs. Figure 5c shows representative nIR images showing nIRCat labeling as well as an overlay depicting regions in green where dopamine activity occurs, highlighting this technique's ability to identify spatially distinct regions of dopamine release at a length scale comparable to single neurons. The nIRCat nanosensor response follows the expected time course for a dopamine release event, an abrupt increase in fluorescence when dopamine is released, followed by an exponential decay as dopamine concentrations dissipate through passive (diffusion) and active (dopamine transporter (DAT) reuptake) transport mechanisms (Fig. 5d,e). Analyzing individual regions of release resolved by using nIRCat imaging enables the study of endogenous variability of dopamine release, reuptake kinetics and quantification of the number of putative release sites throughout the striatum. In addition, this protocol can readily be adapted for acute brain slice imaging of other catecholamines, such as norepinephrine, in other brain regions.

We also demonstrate how this protocol can leverage nIRCat nanosensors' unique ability to function in the presence of pharmacological agents that target endogenous dopamine receptors. Box 1 outlines the procedures for how nIRCat nanosensors can be used to measure and quantify variabilities in dopamine release and reuptake kinetics and changes in the number of dopamine active sites in response to various pharmacological agents. Application of dopamine receptor agonists or antagonists to acute brain slices in combination with optical nanosensor monitoring provides researchers with a detailed view of how individual dopamine release sites are affected by pharmacological agents (Fig. 5f–h), providing insights into the heterogeneity of response underlying biological function as well as the potential impact on drug efficacy and the side effects of new therapies. These studies can be applied to the assessments of animal cohorts and subsequently image differences in dopamine modulation in acute brain slices generated from experimental and control cohorts at commensurate time points applicable to behavioral or neurodegenerative animal studies.

Lastly, the non-genetically encoded nature of nIRCat nanosensors allows for the application of this protocol to imaging dopamine modulation in acute brain slices generated from other animal subjects, including animals too young for genetic manipulation or species that are genetically intractable, expanding the scope of dopamine modulation studies.

Supplementary Material

Refer to Web version on PubMed Central for supplementary material.

Acknowledgements

The authors acknowledge prior work from A.G.B. presented in this protocol and previously published by Beyene et al.[19]. We acknowledge support of NIH MIRA award R35 (to M.P.L.), a Burroughs Wellcome Fund Career Award at the Scientific Interface (CASI) (to M.P.L.), the Simons Foundation (to M.P.L.), a Stanley Fahn PDF Junior Faculty Grant with Award No. PF-JFA-1760 (to M.P.L.), a Beckman Foundation Young Investigator Award (to M.P.L.), a CZI Deep-Tissue Imaging Award (to M.P.L.) and a DARPA Young Investigator Award (to M.P.L.). M.P.L. is a Chan Zuckerberg Biohub investigator. S.J.Y. acknowledges the support of NSF Graduate Research Fellowships (NSF DGE 1752814). J.T.D.B.-O. is supported by the Department of Defense office of the Congressionally Directed Medical Research Programs (CDMRP) Parkinson's Research Program (PRP) Early Investigator Award.

Data availability

All materials are available from commercial sources or can be derived by using methods described in this protocol. All primary data underlying the figures reported in the article are publicly available via the Dryad repository at https://doi.org/10.6078/D1VH87. Additional data can be obtained from the corresponding author upon reasonable request.

References

1. Cohen JY, Haesler S, Vong L, Lowell BB & Uchida N Neuron-type-specific signals for reward and punishment in the ventral tegmental area. Nature 482, 85–88 (2012). [PubMed: 22258508]
2. Double KL & Crocker AD Dopamine receptors in the substantia nigra are involved in the regulation of muscle tone. Proc. Natl. Acad. Sci. USA 92, 1669–1673 (1995). [PubMed: 7878037]
3. Berke JD What does dopamine mean? Nat. Neurosci 21, 787–793 (2018). [PubMed: 29760524]
4. Dudman JT & Krakauer JW The basal ganglia: from motor commands to the control of vigor. Curr. Opin. Neurobiol 37, 158–166 (2016). [PubMed: 27012960]
5. Lebowitz JJ & Khoshbouei H Heterogeneity of dopamine release sites in health and degeneration. Neurobiol. Dis 134, 104633 (2020). [PubMed: 31698055]
6. Bibb JA et al. Severe deficiencies in dopamine signaling in presymptomatic Huntington's disease mice. Proc. Natl. Acad. Sci. USA 97, 6809–6814 (2000). [PubMed: 10829080]
7. Weinstein JJ et al. Pathway-specific dopamine abnormalities in schizophrenia. Biol. Psychiatry 81, 31–42 (2017). [PubMed: 27206569]
8. Greengard P The neurobiology of slow synaptic transmission. Science 294, 1024–1030 (2001). [PubMed: 11691979]
9. Rice ME & Cragg SJ Dopamine spillover after quantal release: rethinking dopamine transmission in the nigrostriatal pathway. Brain Res. Rev 58,, 303–313 (2008). [PubMed: 18433875]
10. Zoli M et al. The emergence of the volume transmission concept. Brain Res. Rev 26, 136–147 (1998). [PubMed: 9651506]
11. Beyene AG, McFarlane IR, Pinals RL & Landry MP Stochastic simulation of dopamine neuromodulation for implementation of fluorescent neurochemical probes in the striatal extracellular space. ACS Chem. Neurosci 8, 2275–2289 (2017). [PubMed: 28714693]
12. Beyene AG, Yang SJ & Landry MP Review article: tools and trends for probing brain neurochemistry. J. Vac. Sci. Technol. A 37, 040802 (2019). [PubMed: 31235991]

13. Chefer VI, Thompson AC, Zapata A & Shippenberg TS Overview of brain microdialysis. Curr. Protoc. Neurosci *Chapter* 7, Unit 7.1 (2009).
14. Nakatsuka N & Andrews AM Differentiating siblings: the case of dopamine and norepinephrine. ACS Chem. Neurosci 8, 218–220 (2017). [PubMed: 28177214]
15. Ngo KT, Varner EL, Michael AC & Weber SG Monitoring dopamine responses to potassium ion and nomifensine by in vivo microdialysis with online liquid chromatography at one-minute resolution. ACS Chem. Neurosci 8, 329–338 (2017). [PubMed: 28094974]
16. Sames D, Dunn M, Karpowicz RJ & Sulzer D Visualizing neurotransmitter secretion at individual synapses. ACS Chem. Neurosci 4, 648–651 (2013). [PubMed: 23862751]
17. Patriarchi T et al. Ultrafast neuronal imaging of dopamine dynamics with designed genetically encoded sensors. Science 360, eaat4422 (2018). [PubMed: 29853555]
18. Sun F et al. A genetically encoded fluorescent sensor enables rapid and specific detection of dopamine in flies, fish, and mice. Cell 174, 481–496.e19 (2018). [PubMed: 30007419]
19. Beyene AG et al. Imaging striatal dopamine release using a nongenetically encoded near infrared fluorescent catecholamine nanosensor. Sci. Adv 5, eaaw3108 (2019). [PubMed: 31309147]
20. Hong G et al. Through-skull fluorescence imaging of the brain in a new near-infrared window. Nat. Photonics 8, 723–730 (2014). [PubMed: 27642366]
21. O'Connell MJ et al. Band gap fluorescence from individual single-walled carbon nanotubes. Science 297, 593–596 (2002). [PubMed: 12142535]
22. Beyene AG et al. Ultralarge modulation of fluorescence by neuromodulators in carbon nanotubes functionalized with self-assembled oligonucleotide rings. Nano Lett 18, 6995–7003 (2018). [PubMed: 30350638]
23. Jeong S et al. High-throughput evolution of near-infrared serotonin nanosensors. Sci. Adv 5, 3771–3789 (2019).
24. Li C & Wang Q Challenges and opportunities for intravital near-infrared fluorescence imaging technology in the second transparency window. ACS Nano 12, 9654–9659 (2018). [PubMed: 30347984]
25. Kruss S et al. High-resolution imaging of cellular dopamine efflux using a fluorescent nanosensor array. Proc. Natl. Acad. Sci. USA 114, 1789–1794 (2017). [PubMed: 28179565]
26. Dinarvand M et al. Near-infrared imaging of serotonin release from cells with fluorescent nanosensors. Nano Lett 19, 6604–6611 (2019). [PubMed: 31418577]
27. Del Bonis-O'Donnel JT et al. Engineering molecular recognition with bio-mimetic polymers on single walled carbon nanotubes. J. Vis. Exp 119, 55030 (2017).
28. Zhang J et al. Molecular recognition using corona phase complexes made of synthetic polymers adsorbed on carbon nanotubes. Nat. Nanotechnol 8, 959–968 (2013). [PubMed: 24270641]
29. Boyden ES, Zhang F, Bamberg E, Nagel G & Deisseroth K Millisecond-timescale, genetically targeted optical control of neural activity. Nat. Neurosci 8, 1263–1268 (2005). [PubMed: 16116447]
30. Kida H, Sakimoto Y & Mitsushima D Slice patch clamp technique for analyzing learning-induced plasticity. J. Vis. Exp 129, 55876 (2017).
31. Geiger BM, Frank LE, Caldera-Siu AD & Pothos EN Survivable stereotaxic surgery in rodents. J. Vis. Exp 20, 880 (2008).
32. Romano SA et al. An integrated calcium imaging processing toolbox for the analysis of neuronal population dynamics. PLoS Comput. Biol 13, e1005526 (2017). [PubMed: 28591182]
33. Pnevmatikakis EA et al. Simultaneous denoising, deconvolution, and demixing of calcium imaging data. Neuron 89, 285–299 (2016). [PubMed: 26774160]
34. Jeng ES-H The Investigation of Interactions between Single Walled Carbon Nanotubes and Flexible Chain Molecules. Thesis, Massachusetts Institute of Technology (2010).
35. Schneider CA, Rasband WS & Eliceiri KW NIH Image to ImageJ: 25 years of image analysis. Nat. Methods 9,, 671–675 (2012). [PubMed: 22930834]
36. Schindelin J et al. Fiji: an open-source platform for biological-image analysis. Nat. Methods 9,, 676–682 (2012). [PubMed: 22743772]

37. Van Der Walt S et al. scikit-image: image processing in Python. PeerJ 2, e453 (2014). [PubMed: 25024921]

38. Otsu N Threshold selection method from gray-level histograms. IEEE Trans. Syst. Man Cybern SMC-9, 62–66 (1979).

39. Sorensen J, Wiklendt L, Hibberd T, Costa M & Spencer NJ Techniques to identify and temporally correlate calcium transients between multiple regions of interest in vertebrate neural circuits. J. Neurophysiol 117, 885–902 (2017). [PubMed: 27903638]

Box 1 | Imaging nIRCat in brain slices by using drug washes ● Timing ~1 h per acute brain slice

This box describes how to adapt the standard acute brain slice imaging protocol (Steps 55–63) to study how dopamine response changes with the wash-on of pharmaceutical agents such as dopamine receptor agonists and antagonists.

Procedure

1. Prepare drug solutions in freshly prepared ACSF and keep the ACSF-drug mixture refrigerated until use.

   ▲ **CRITICAL STEP** All new drug solutions should be checked beforehand in in vitro solution-phase experiments to ensure that they do not elicit an optical response from nIRCat in the absence of dopamine. nIRCat has been validated not to respond optically to the D2R antagonists sulpiride and haloperidol, the D2R agonist quinpirole or the D1R antagonist SCH 23390.

2. Depending on the stimulation method desired, follow the aforementioned methods for electrical or optogenetic stimulation (Steps 55–58) to find a field of view for imaging. Collect baseline drug-free data as described in Steps 58–62 by continuously perfusing normal ACSF in the microscope perfusion chamber.

3. To collect drug-wash data, switch the perfusion system to flow carbogen-bubbled drug ACSF solution into the microscope perfusion chamber. Allow the drug solution to occupy the microscope perfusion chamber for 10 min. The exact timing of drug solution exposure needed to reach desired effects will vary on the basis of the microscope perfusion system, the concentration of drug and the type of drug being applied. Adjust the drug exposure time as needed for the desired experimental parameters.

4. Keep perfusing the perfusion system with the drug solution. Stimulate the slice and collect time series by using the same protocol as used for the drug-free data described in Steps 58–62.

5. To collect drug wash-off data, switch the perfusion system to flow carbogen-bubbled drug-free ACSF into the perfusion chamber. Stimulate the slice and collect time series data by using the same protocol used for the drug-free and drug-wash data.

   ▲ **CRITICAL STEP** We found that some drugs can persist in perfusion lines and contaminate subsequent experiments. Ensure that all tubing, baths, reservoirs and beakers are thoroughly cleaned or replaced between sensitive experiments.

6. Proceed to Step 63 of the main procedure for post-experiment microscope cleaning.

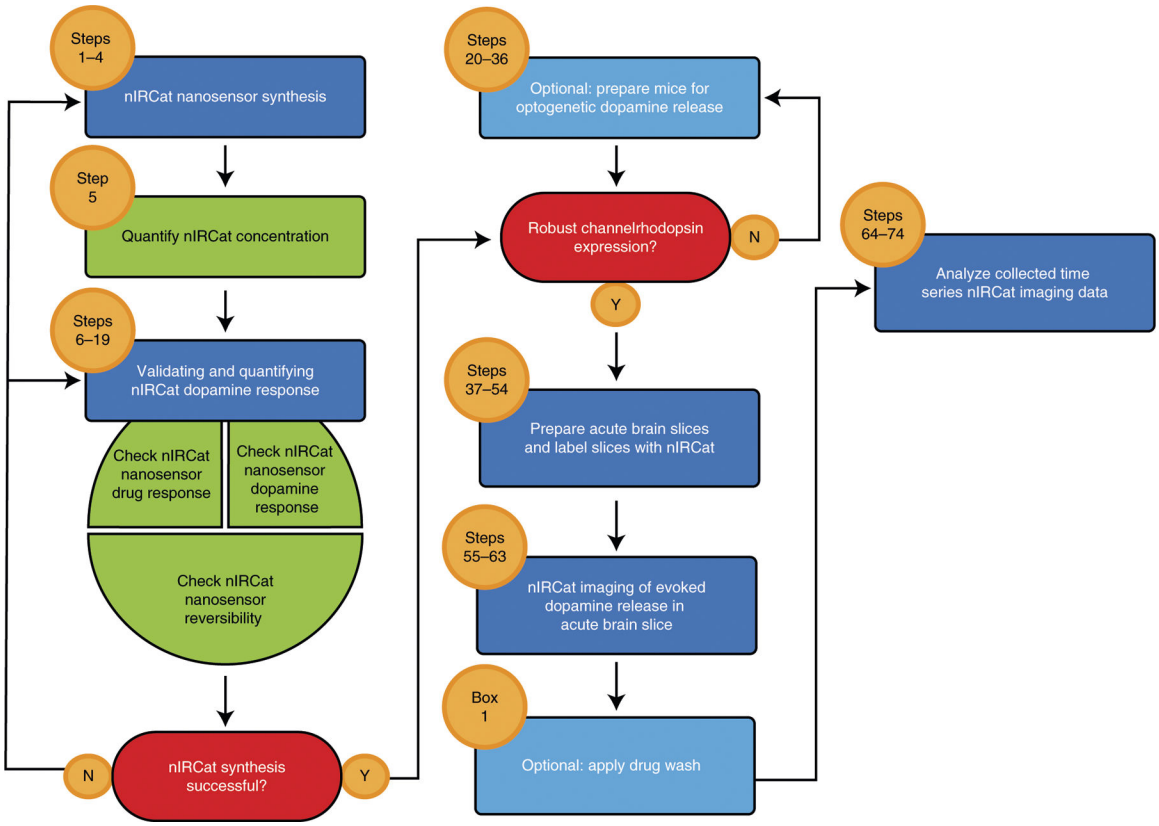

Fig. 1 |. Overview of the procedure.

Experimental flow chart of described protocols. Column 1 describes steps relevant to nIRCat nanosensor synthesis. Column 2 describes steps relevant to nIRCat imaging in acute brain slices. Column 3 describes steps relevant to time series nIRCat imaging data. Dark blue boxes represent experimental steps, whereas light blue boxes represent additional experimental steps that can be added or removed depending on the planned experiment. Green boxes represent characterization steps, and red boxes represent checkpoint steps. N, no; Y, yes.

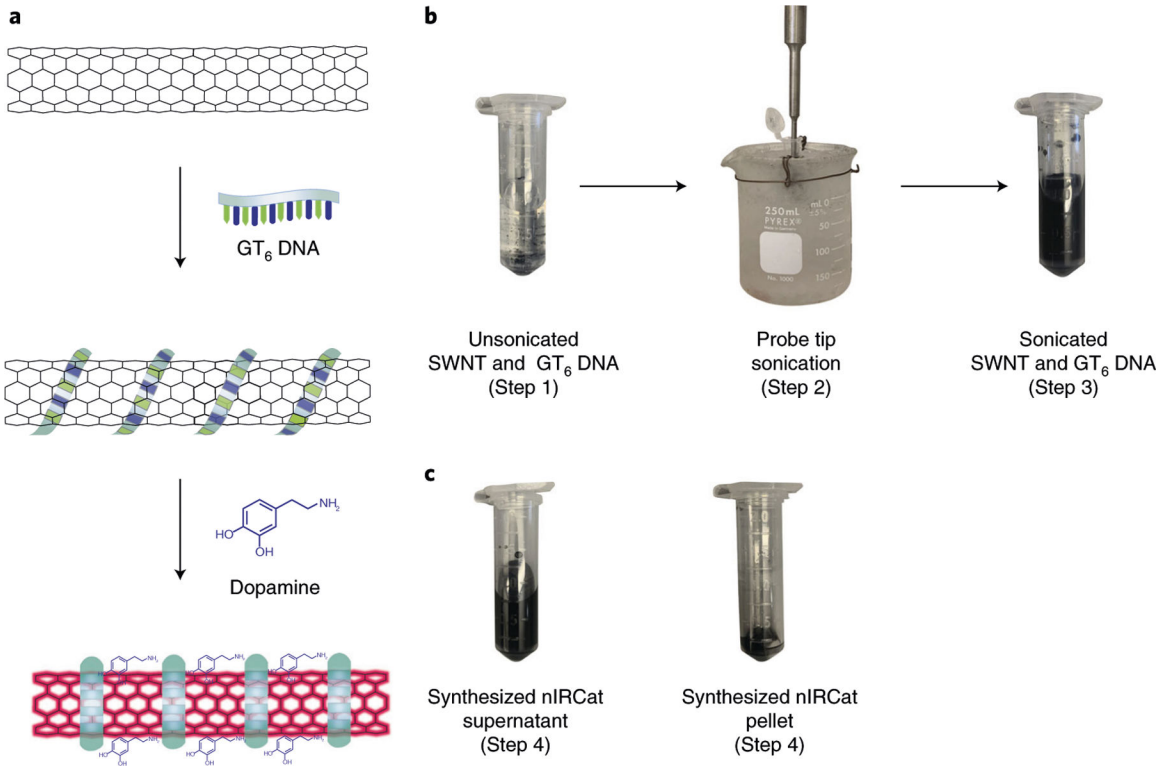

Fig. 2 |. nIRCat synthesis.

a, Schematic representation of the nIRCat synthesis process. SWNTs are sonicated with single-stranded GT_6 DNA, resulting in an assembled SWNT-DNA complex. This complex is the nIRCat and shows an increase in fluorescence in the presence of dopamine. **b**, Before sonication, the SWNTs should appear as dark non-dispersed particles in solution. To sonicate the solution, form a tube holder by using copper wire and place the solution in a microcentrifuge tube, immersed in an ice bath. After sonication, the solution should appear dark and relatively uniform. **c**, After centrifugation, the SWNT-DNA solution should still remain dark in color. Remove ~90% of the synthesized nIRCat supernatant and store at 4 °C. Leave the pellet undisturbed and discard as chemically hazardous waste.

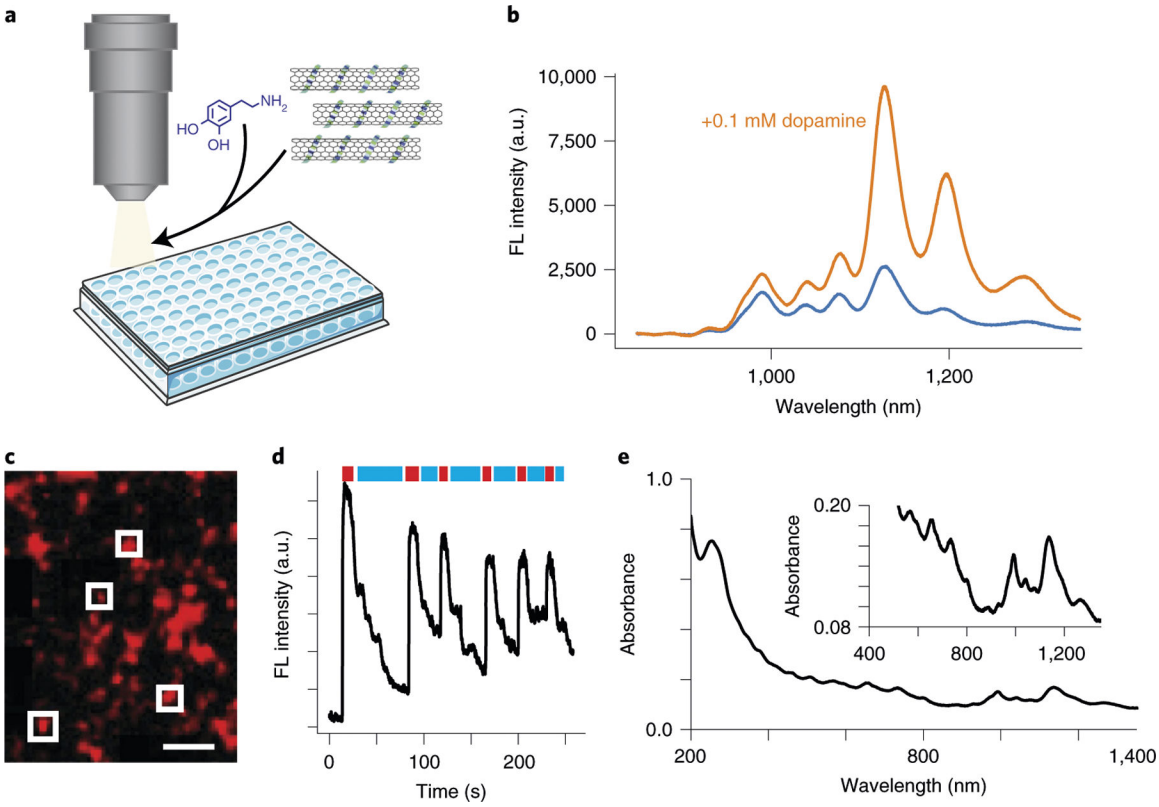

Fig. 3 |. nIRCat characterization.

a, Schematic representation of the nIRCat characterization process. The nIRCat dopamine response can be assessed by an imaging sensor combined with fresh dopamine-HCl solution in a well plate. **b**, Representative fluorescence response from synthesized nIRCat[29]. The blue trace shows nIRCat fluorescence emission before adding dopamine. The orange trace shows nIRCat fluorescence after addition of 0.1 mM dopamine HCl. **c**, nIR fluorescence images of individual nIRCat nanosensors on the surface of a coverslip. Squares denote individual nIRCats. Scale bar = 5 μm. **d**, Relative fluorescence intensity of surface-immobilized nIRCats as 0.1 mM dopamine-HCl solution is washed on and off the surface by using a flow cell and syringe pump, demonstrating nanosensor reversibility. **e**, Absorbance spectrum for a solution of nIRCat nanosensors showing absorbance peaks corresponding to ssDNA and the E_{11} and E_{22} SWNT electronic transitions. Inset: Rescaled for clarity. FL, fluorescence.

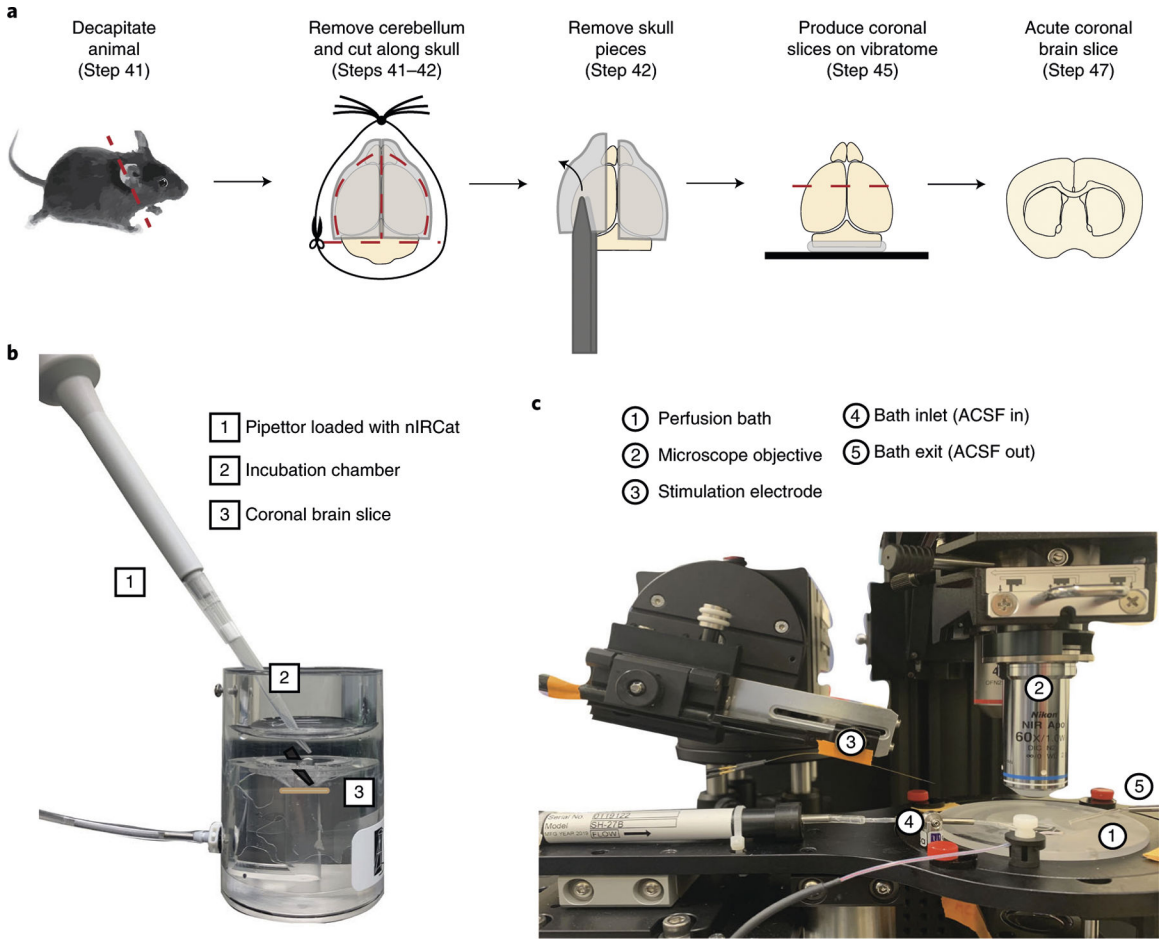

Fig. 4 |. Preparation of nIRCat-labeled acute brain slices.

a, Schematic representation of the dissection process for the generation of acute coronal brain slices. Red dashed lines represent areas to be cut by using scissors or a vibratome. **b** Incubation set up to label acute brain slices with nIRCat. **c**, Microscope perfusion bath set up to image nIRCat-labeled acute brain slices. Coronal brain slices should be placed in the perfusion bath (circle 1) and weighed down by a harp. Acute slices should be placed with the nIRCat-labeled side facing toward the microscope objective.

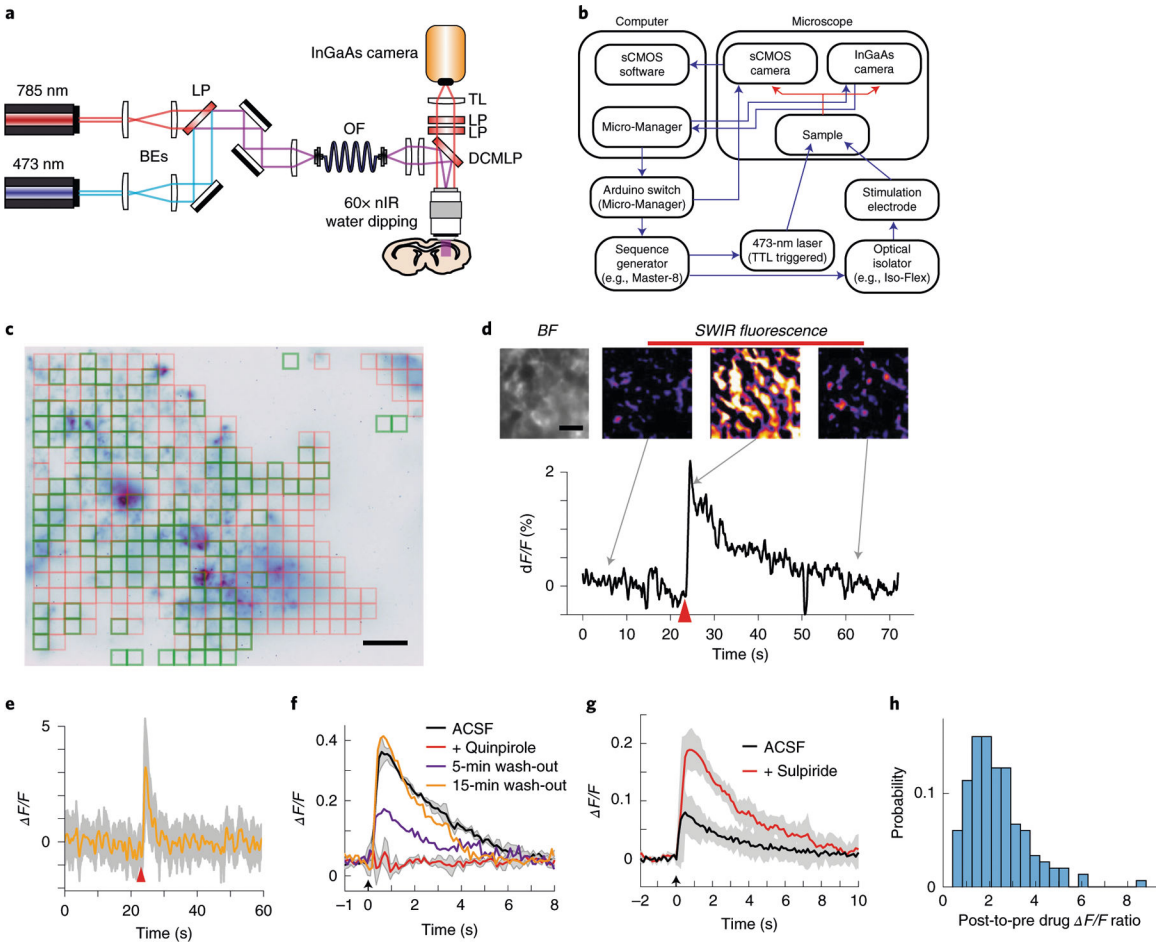

Fig. 5 |. Acquiring and processing evoked dopamine response from nIRCat-labeled acute brain slices.

a, Schematic depicting the arrangement of optical components in an nIRCat imaging system. Laser light is beam-expanded and combined into a multimode optical fiber and then focused to the back focal plane of an nIR-compatible objective. Fluorescence emitted by the sample is re-collected and passed through 900-nm long-pass filters and additional cleanup filters. The transmitted fluorescence is focused by a tube lens onto the InGaAs camera sensor. **b**, Schematic depicting the microscope control and automation of time series image acquisitions and stimulations of acute brain slices. **c**, Representative nIR image of dorsal striatum obtained from an nIRCat-labeled mouse acute brain slice. Square ROIs depict regions where baseline fluorescence was above a threshold value. Squares outlined in red exhibited a negligible fluorescence transient after stimulation, whereas those outlined in green were identified as ‘active’ regions with a statistically significant transient associated with dopamine release. Scale bar = 20 μm. **d**, Representative brightfield (BF) image and nIR fluorescence images showing the increase in relative fluorescence (Δ*F*/*F*) in response to dopamine release evoked by an electrical stimulation (red triangle). Scale bar = 10 μm. **e**, Δ*F*/*F* trace averaged over all ‘active’ regions (orange) with standard deviation bounds (gray). **f** and **g**, Representative results demonstrating that nIRCat nanosensor fluorescence reflects the changes to dopamine release induced by 1 μM D2 agonist quinpirole **f** and D2

antagonist sulpiride (**g**). **h**, A histogram depicting the regional heterogeneity of sulpiride's impact on dopamine release for individual ROIs (~2-μm diameter). BE, beam expander, DCMLP, dichroic long-pass mirror; LP, long-pass filter; OF, optical fiber; TL, tube lens. Plots in **f–h** were adapted from ref. [19].

Table 1 |

Troubleshooting table

Step	Problem	Possible reason	Solution
4	A large amount of nIRCat crashes out of the supernatant and into the pellet, such that the concentration of suspended nIRCat recovered in the supernatant is low	The probe tip was not properly submerged in the SWNT-DNA solution The SWNT-DNA solution was not properly cooled during probe tip sonication	Ensure that the probe tip is placed in the center of the microcentrifuge tubes and is not touching the tube wall Check the ice bath throughout the sonication process and add new ice if necessary
		The nIRCat nanosensor was not created with an optimal SWNT to GT_6 ssDNA ratio	Take care to measure out an accurate amount of dry SWNT before sonication. If problems persist, increase the amount of SWNT while holding the ssDNA quantity constant to make achieving the correct ratio easier
8	The nIRCat nanosensor does not show a robust response to dopamine	The dopamine-HCl solution has oxidized	Prepare fresh 1 mM dopamine-HCl solution right before testing the nanosensor response
		The nIRCat nanosensor was not synthesized properly	Check to see if the synthesized nIRCat achieved proper suspension with a concentration of ≥20 mg/liter in the supernatant. If not, troubleshoot by using the suggestions presented above for Step 4
9	The nIRCat nanosensor shows an optical response to a drug of interest	The drug of interest is too structurally similar to dopamine	Use a drug analog that is more structurally distinct from dopamine
47	The generated acute brain slices are not viable or have many dead cells	The vibratome speed and frequency are too fast or slow	Speed and frequency settings will depend on the particular vibratome. We suggest a nominal cut speed of 0.05 mm/s as a starting point. Increase the frequency until the cutting blade no longer pushes and deforms the brain tissue
		The brain was not kept submerged in cooled cutting buffer during dissection	Keep the brain submerged in cold cutting buffer for the duration of dissection. In addition, the dissection process should be completed as efficiently as possible, ideally within 15 min
		The cutting buffer was not properly oxygenated with carbogen	Ensure that the cutting buffer is bubbled for ≥10 min before perfusion. Maintain a steady bubbling of cutting buffer throughout the dissection and cutting process
59	Imaging on High Gain results in ‘hot pixels’ that saturate easily	The camera settings result in ‘hot pixels’	Collect the image as intended and remove the ‘hot pixels’ in post-processing
60	Acute brain slices shows poor nIRCat labeling	The more strongly labeled face of the slice is not facing the objective The nIRCat nanosensor has crashed out of solution or has degraded	Using a transfer pipette, flip the slice so that the more strongly labeled face points toward the objective Test the nIRCat nanosensor in in vitro solution-phase experiments to verify a robust dopamine response (Steps 7–11). If the nanosensor is degraded, synthesize a new batch. The nanosensor should be stored at 4 °C to prevent degradation
	Image collection shows significant motion that confounds later data processing	The harp is not properly anchoring the slice The pump for the microscope perfusion system is ‘hiccupping’ and alternating between expelling and intaking ACSF from the bath ACSF entering or leaving the bath is disturbing the slice A bubble is being formed at the electrode tip during stimulation	Adjust the harp so that it lies flat on the acute brain slice. Take care to ensure that the harp is not stuck on the edge of the perfusion bath and does not have loose strings Adjust the tubing in the peristaltic pump to ensure that it is not catching and producing a ‘hiccup’. Flush the perfusion system by using a syringe to check for salt build-up. The perfusion system should always be rinsed with distilled water after use to prevent salt buildup Adjust the inlet and outlet points around the bath to ensure that the slice is minimally affected by the perfusion system. Adjust the ACSF flow rate if needed To minimize bubble formation, researchers can use low-impedance electrodes (e.g., platinum electrodes vs tungsten electrodes). Researchers can also decrease the delivered stimulation intensity or switch to a stimulation train